HHS Public Access

Author manuscript

Mol Cell Neurosci. Author manuscript; available in PMC 2017 September 01.

Published in final edited form as:

Mol Cell Neurosci. 2016 September ; 75: 14–26. doi:10.1016/j.mcn.2016.06.002.

The Rac-GAP alpha2-chimaerin regulates hippocampal dendrite and spine morphogenesis

Chris M. Valdez[a], **Geoffrey G. Murphy**[a,b], and **Asim A. Beg**[a,c,*]

[a]Interdepartmental Program in Neuroscience, University of Michigan, Ann Arbor, MI 48109, United States

[b]Molecular and Behavioral Neuroscience Institute, Department of Molecular and Integrative Physiology, University of Michigan, Ann Arbor, MI 48109, United States

[c]Department of Pharmacology, University of Michigan, Ann Arbor, MI 48109, United States

Abstract

Dendritic spines are fine neuronal processes where spatially restricted input can induce activity-dependent changes in one spine, while leaving neighboring spines unmodified. Morphological spine plasticity is critical for synaptic transmission and is thought to underlie processes like learning and memory. Significantly, defects in dendritic spine stability and morphology are common pathogenic features found in several neurodevelopmental and neuropsychiatric disorders. The remodeling of spines relies on proteins that modulate the underlying cytoskeleton, which is primarily composed of filamentous (F)-actin. The Rho-GTPase Rac1 is a major regulator of F-actin and is essential for the development and plasticity of dendrites and spines. However, the key molecules and mechanisms that regulate Rac1-dependent pathways at spines and synapses are not well understood. We have identified the Rac1-GTPase activating protein, α2-chimaerin, as a critical negative regulator of Rac1 in hippocampal neurons. The loss of α2-chimaerin significantly increases the levels of active Rac1 and induces the formation of aberrant polymorphic dendritic spines. Further, disruption of α2-chimaerin signaling simplifies dendritic arbor complexity and increases the presence of dendritic spines that appear poly-innervated. Our data suggests that α2-chimaerin serves as a “brake” to constrain Rac1-dependent signaling to ensure that the mature morphology of spines is maintained in response to network activity.

Keywords

Dendrites; Spines; Synapse; Chimaerin; Long-term potentiation

1. Introduction

Nervous system function relies on the precise wiring of neuronal circuits during development (Goodman and Shatz, 1993). A key parameter in this process is the elaboration

*Corresponding author at: University of Michigan, 1150 W. Medical Center Dr., 1301D MSRB III, Ann Arbor, MI 48109, United States., asimbeg@umich.edu (A.A. Beg).

Conflict of interest

The authors declare no competing financial interests.

of axonal and dendritic arbors, as their size and complexity determines the number of synaptic connections a neuron makes and receives, respectively (Hausser et al., 2000). With billions of neurons in the brain making trillions of synapses, individual axons and dendrites have the momentous task of locating the appropriate partner(s) in which to form synaptic connections. The majority of excitatory synaptic neurotransmission occurs at dendritic spines, the tiny filamentous (F)-actin rich protrusions that emanate from dendritic shafts (Harris, 1999; Matus, 2000). A typical dendritic spine contains a single glutamatergic synapse, thus spine density reflects the amount of excitatory drive a neuron receives (Fiala et al., 2002). Moreover, spines are highly modifiable and exhibit tremendous structural and functional plasticity. Structural plasticity involves cytoskeletal rearrangement that affects spine morphology; whereas, functional plasticity leads to changes in glutamate receptor efficacy (Fischer et al., 2000; Segal and Andersen, 2000). These changes in spine shape and number can last for weeks in vivo and are thought to reflect cellular mechanisms underlying cognitive processes like learning and memory (Bhatt et al., 2009). Not surprisingly, mutations in signaling pathways that regulate F-actin cause abnormalities in dendritic spine shape, density and function; pathological hallmarks highly correlated with neurodevelopment, neuropsychiatric and neurodegenerative disorders (Penzes et al., 2011).

In response to physiological stimuli, a complex network of signaling events can trigger changes in dendritic spine number and morphology. Rho-GTPases are key proteins that regulate actin cytoskeletal dynamics by coupling upstream signals with the correct downstream effector proteins (Hall, 1998; Luo, 2000). Rho-GTPases control diverse cellular processes; thus, signaling specificity is achieved through regulatory proteins that modulate the spatiotemporal activity of Rho-GTPases (Cherfils and Zeghouf, 2013). Like all Rho-GTPases, Rac1 acts a molecular switch cycling between a GDP-bound inactive form and a GTP-bound active form. Rac1 is activated by guanine exchange factors (GEFs) and inactivated by GTPase-activating proteins (GAPs) (Bos et al., 2007). Despite the importance of these regulatory factors, it is unclear how GEFs and GAPs coordinately act to regulate Rac1 signaling in dendrites and spines. Moreover, few essential Rac-GAP proteins have been identified that transduce synaptic activity to Rac1 inactivation.

Here, we demonstrate that the Rac-GAP α2-chimaerin plays an important role in hippocampal dendrite arborization and spine morphogenesis. Our findings reveal that α2-chimaerin is a major negative regulator of Rac1 whose loss simplifies hippocampal dendritic arbor complexity, decreases dendritic spine protrusion density, alters spine morphology, and increases the density of polysynaptic dendritic spines; but, is dispensable for long-term potentiation at CA3-CA1 hippocampal synapses. Together, these data provide important insight into the molecular repertoire that shapes dendrites, spines and synapses. Importantly, our data identify α2-chimaerin as a novel Rac-GAP protein that plays a key role in counterbalancing GEF activation of Rac1 in spines and synapses.

2. Materials and methods

2.1. Animal strains, ethics and welfare

Animals were housed and handled in accordance with the guidelines from the National Institutes of Health and the Institutional Animal Care and Use Committee (IACUC) at the

University of Michigan. Mice were housed in a 12 h light-dark cycle with food and water ad libitum. Mice containing a gene-trap insertion in the α-chimaerin gene ($\alpha2^{gt/gt}$) were obtained from Lexicon Genetics as previously described (Beg et al., 2007). For in vivo dendritic arborization analyses, α2-chimaerin genetrap mice were bred with Thy1-GFP-M transgenic mice (Feng et al., 2000). The wild type strain used in this study (C57BL/6 J) were obtained from Jackson Laboratories (Bar Harbor, ME).

2.2. Lentiviral production and shRNA constructs

Phosphorylated duplex shRNA oligonucleotides were ligated into the HpaI/XhoI sites of a modified pLL3.7 (Addgene #11795), in which mApple expression is driven by the CMV promoter. Target sequences were as follows: *scramble*, 5′-GTTCATATGTTCACCTATT-3′; *sh1*, 5′-GCACATGGCAGTCCTGAAA-3′; *sh2*, 5′-GCAGCAGAATACATTGCCA-3′; *sh3*, 5′-GTACACTTTGGCTTTAAGA-3′. To determine shRNA knockdown efficacy, a murine *N*-terminal-tagged HA::α2-chimaerin plasmid (500 ng) was transfected alone or co-transfected with individual shRNA (500 ng) constructs into HEK-293 T cells using LipoD293 (SignaGen). To determine specificity, an shRNA resistant HA::α2-chimaerin plasmid was created in which each shRNA target site sequence was mutated by at least 4 nucleotides. A murine HA::α1-chimaerin plasmid was co-transfected with each shRNA to determine the extent of off-target α1-chimaerin knockdown. The extent and specificity of knockdown was determined by analyzing whole-cell protein lysate (10 μg) 48 h post-transfection using SDS-PAGE and immunoblotting. Lentiviral particle production was performed as previously described using 2nd generation plasmids (Addgene: pMD2G, #12259; psPAX2, #1260) (Ellis et al., 2011). Seventy-two hours after transfection, lentiviral supernatants were harvested and concentrated by spinning at 20,000 relative centrifugal force (r.c.f) for four hours at 4 ° C. Pelleted lentivirus was resuspended in 100 μl 1× PBS, aliquoted and flash frozen. Lentiviral titers were determined using a qRT-PCR based approach (ABM, LV900). At 5 DIV, an MOI of 10 was used to infect primary hippocampal cultures (500,000 cells/35 mm dish, N = 3 experimental replicates/condition, n = 3 dishes/condition). After 6 days, neurons were lysed in RIPA buffer and 20 μg of protein was separate by SDS-PAGE and proteins were immunoblotted using an *anti*-CHN1 antibody to assess endogenous α2-chimaerin protein levels, and GAPDH as a loading control.

2.3. Primary cell cultures

P0–1 C57BL/6 J (WT) and α2-chimaerin genetrap homozygous mutant ($\alpha2^{gt/gt}$) pups were used to prepare primary hippocampal neuronal cultures as previously described (Kaech and Banker, 2006). Briefly, hippocampi were microdissected in Hanks-buffered salt solution (HBSS) without $MgCl_2$ and $CaCl_2$ containing 10 mM HEPES. Isolated hippocampi were incubated with 0.25% Trypsin + 0.01% DNaseI in HBSS + 10 mM HEPES solution for 15 min at 37 °C. Tissue was washed with 5 mL of culture media containing DMEM (Gibco 11,995-065), 0.8% D(+)Glucose, 1% Glutamax and 10% FBS. Hippocampi were triturated to a single cell suspension in 1 mL of media with a glass pasteur pipette. The cell suspension was pelleted for three minutes (1500 rotations per minute (r.p.m.). Culture media was removed and the cell pellet was re-suspended to a single cell suspension in 1 mL of fresh culture media. Cells were counted using Trypan Blue exclusion. Approximately 50,000 cells were seeded in plating media on 12 mm glass-coated coverslips (poly-*D*-lysine, 50 μg/μL) in

24-well plates or on 35 mm μ-dishes (Ibidi, 81,156). After three hours, plating media was replaced with neuronal maintenance media containing Neurobasal, 1× B27 and 1× Glutamax. After two days, neurons were treated with 2 μM cytosine d-D-arabinofuranoside (AraC). Every 3–4 days, 50% of the media was replaced with fresh neural growth media.

2.4. Transfections

2.4.1. α2-chimaerin localization—To assess the subcellular localization of α2-chimaerin, primary wild type (WT) neurons were co-transfected with 550 ng of a β-actin-mCherry plasmid (pCAG-mCherry-WPRE) and 50 ng of an EGFP::α2-chimaerin plasmid as previously described (Buttery et al., 2006). Neurons were incubated with the transfection complexes for 2 h in a 37 °C/5%CO_2 incubator, and the transfection media was subsequently replaced with neuronal maintenance media described above. Neurons were transfected at 16 DIV and fixed at 18 DIV using 4% paraformaldehyde for 10 min. Fixed neurons were subsequently washed three times in 1× PBS and mounted onto glass slides with Fluoromount-G (Southern Biotech).

2.4.2. Dendritic morphology and synapse quantitation—To analyze dendritic arborization, spine morphology and putative synaptic contacts, WT and α2-chimaerin mutant hippocampal neurons were transfected at 10 DIV. Transfection complexes were made by mixing 0.5 μL of Lipofectamine 2000 (Life Technologies) with 500 ng of a β-actin-GFP plasmid (pCAG-EGFP-WPRE), per well of a 24-well plate. Between 16 and 18 DIV, the transfected hippocampal neurons were fixed (4% paraformaldehyde, 10 min) for morphological analysis or immunostained with the excitatory synaptic markers synaptophysin and PSD-95.

2.4.3. F-actin quantitation—Primary hippocampal cultures (10 DIV) were transfected with pCAG-EGFP-WPRE plasmids as described above. At 16–18 DIV, cells were fixed and stained with Alexa594-Phalloidin (1:1000, Cytoskeleton Inc.) for 1 h at room temperature. For each experimental set (N = 3), confocal laser power and gain were adjusted such that <1% of pixels were saturated for WT neurons. These settings were subsequently used to image both WT and $\alpha2^{gt/gt}$ mutant neurons for each experimental set. Pooled data from the three experimental sets were averaged and analyzed using and unpaired two-tailed test.

2.4.4. Single cell knockdown—At 10 DIV, primary WT hippocampal neurons were co-transfected with 100 ng of control (*scramble*) or an α2-chimaerin-specific shRNA (*sh2*) plus 500 ng of pCAG-EGFP-WPRE plasmid. Between 16 and 18 DIV, the neurons were fixed and dendritic structures were analyzed using confocal microscopy. The *sh2* construct was used for all experiments as it demonstrated the highest knockdown efficacy.

2.4.5. Single cell re-expression—At 10 DIV, primary WT and α2-chimaerin mutant hippocampal neurons were co-transfected with 300 ng of pCAG-EGFP-WPRE (control) and 300 ng pBluescriptII plasmid, or with 300 ng EGFP::α2-chimaerin and 300 ng pCAG-EGFP-WPRE plasmids using 0.5 μL of Lipofectamine 2000 (Life Technologies). At 16 DIV, neurons were fixed and dendritic structures were analyzed using confocal microscopy.

2.5. Rac1-GTP G-LISA

Primary hippocampal cultures were plated at a density of 500,000 cells per 35 mm dish. After 18–20 DIV, cells were lysed and protein concentration was determined. Equivalent amounts of protein lysate were loaded to assess Rac1-GTP levels using the G-LISA colorimetric assay (Cytoskeleton, Inc.). Four WT and α2-chimaerin mutant experimental sets were utilized to prepare eight 35 mm dishes containing 500,000 primary neurons (2 dishes/experimental set). The OD values from each experimental set were averaged and the mean difference between genotypes was statistically evaluated by a paired two-tailed *t-test*, $\alpha = 0.05$. A detailed protocol can be found at www.cytoskeleton.com/bk128.

2.6. Immunocytochemistry

Between 16 and 18 DIV, primary neurons were fixed with 4% paraformaldehyde (PFA)/4% sucrose in Dulbecco's phosphate buffer containing $MgCl_2$ and $CaCl_2$ (DPBS-MC) for 15 min at room temperature (RT). After fixation, coverslips were washed three times in DPBS-MC and permeabilized in 0.01% TritonX-100 for ten minutes at RT. Cells were washed three times after permeabilization and then incubated in 10% Donkey serum for 30 min at 4 °C in a humidifying chamber. Blocked coverslips were incubated with primary antibodies overnight at 4 °C in a humidified chamber, washed three times with DPBS-MC for five minutes each at RT, and then incubated in fluorescent secondary antibodies for 60 min at RT in a humidifying chamber. Coverslips were washed and mounted on glass slides with Fluoromount-G (Southern Biotech).

2.7. Antibodies

PSD-95 (NeuroMab clone K28/43); Synaptophysin (Millipore 04-1019); anti-CHN1 (abcam156869); GAPDH (GeneScript A00191-40); and anti-HA (Roche clone 3F10) were used for immunoblotting and immunofluorescence. For immunofluorescence, Alexa488, 594, 647-conjugated secondary antibodies (Jackson Immunoresearch) were used at 1:1000 dilution for 1 h at room temperature.

2.8. Dendritic arborization image analysis

To analyze dendritic arborization in primary hippocampal neurons, EGFP positive cells were imaged with a 20× objective on a wide-field fluorescence microscope (Leica DMI6000B). We utilized a semi-automated approach to trace dendritic segments from a single neuron with the NeuroJ Plugin in ImageJ (Meijering, 2010). From the generated binary image, we analyzed dendritic complexity by counting the number of proximal to distal dendritic intersections on concentric circles placed in a 20 μm fixed radius around the soma via the Sholl Analysis Plugin in ImageJ (Longair et al., 2011). For in vivo dendritic arborization analysis, we utilized the same process and quantitative approaches as above; however, single cell images were collected from Z-series confocal micrographs (50 μm slice volume, 0.5 μm step size) that were maximally projected (Nikon A1R).

2.9. Dendritic spine image analysis

Dendritic spine images were collected from Z-series confocal micrographs using a 60× objective with a 3× digital zoom at 1024 $pixel^2$ (Nikon A1R laser scanning confocal

microscope, 0.25 μm step size). The images were maximally Z-projected and then segmented with a line function to straighten 30 μm segments of secondary and tertiary dendrites. The 30 μm straightened dendritic segments were used to analyze spine density and protrusion shape frequencies. The protrusion shapes were binned into three categories essentially as described (Srivastava et al., 2011): 1) filopodial-like protrusions that exhibit a thin protrusion and lack a bulbous-shaped head; 2) dendritic spines, which are divided into; a) stubby spines that are stocky bulbous shaped protrusions; b) mushroom spines that exhibit a narrow neck with a bulbous-like head; and 3) atypical spines which are either bifurcated spines that exhibit a split spine neck and two separate bulbous-like protrusion heads, or branched spines, that resemble mushroom spines with a single or multiple mushroom-shaped protrusions emanating from the primary spine head. For in-vivo protrusion analysis, we counted secondary and tertiary dendritic protrusions on CA1 neurons from WT;Thy1-GFP-M+ and $\alpha 2^{gt/gt}$;Thy1-GFP-M+ mice.

2.10. Synapse imaging analysis

For synapse analysis, primary GFP-transfected neurons were immunostained with synaptophysin to label all pre-synaptic sites, and PSD-95 to label excitatory post-synaptic structures. Z-series confocal micrographs of secondary and tertiary dendrites were collected with a 60× objective plus a 3× digital zoom at 1024 pixel^2, and 30 μm dendritic segments were straightened from the collected images. Putative synaptic contacts were determined by the apposition of synaptophysin and PSD-95 markers. The combination of synaptic marker staining and the EGFP-expressing cells allowed for quantification of synaptic contacts and synapse localization per protrusion-type.

2.11. Atypical branched spine synaptic contacts

The multiplicity of synaptic contacts was determined by quantifying the number of apposed SYN/PSD-95 puncta on a single branched spine. A branched spine was considered monosynaptic if it exhibited a single synaptic contact defined as the apposition of pre- and postsynaptic markers on the primary spine head (spine head that emanates from a spine neck connected to the dendritic shaft). A branched spine was considered polysynaptic if it exhibited two or more synaptic contacts present on 1) the primary head, and 2) a secondary spine head, which extends from a spine neck connected to the primary spine head itself. The analysis was completed from three WT and α2-chimaerin mutant experimental sets. Confocal micrographs were prepared from 28 WT and 24 α2-chimaerin mutant neurons. From these images, the multiplicity of synaptic contacts was analyzed from 45 WT and α2-chimaerin mutant dendritic segments (30 μm). The Fisher's exact two-tailed test was utilized to test if atypical dendritic spines exhibited significant differences in innervation.

2.12. Slice preparation

Mice were anesthetized with isoflurane followed by decapitation to isolate the brain. The cerebellum was removed and the posterior end of the brain was glued to a cutting stage and immediately placed in ice-cold oxygenated artificial cerebrospinal fluid (aCSF in mM: 125 NaCl, 25 NaHCO3, 2.5 KCl, 1.25 NaH2PO4, 2 CaCl2, 1 MgCl2, 0.4 ascorbic acid, and 25 D-glucose). We prepared 400 μm coronal sections at a slicing speed of 0.14 mm/s. and 1.00 mm amplitude using a vibratome (VT1000S, Leica Microsystems). Brain slices containing

the hippocampus were cut at the mid-sagittal line and transferred to a holding chamber filled with oxygenated aCSF. After one hour, the brain slices were individually transferred to a submersion chamber and continuously perfused with oxygenated aCSF at 31 °C.

2.13. Electrophysiology

To examine LTP in the CA3-CA1 hippocampal circuit, recording and stimulating electrodes were placed in the Schaffer Collateral region of CA1. The recording electrode was constructed from a Clark Borosilicate Standard Wall glass pipette pulled from a P-97 Flaming-Brown pipette puller and filled with aCSF. The recording electrode was connected to an amplifier and subsequent recordings were digitized (lowpass filter frequency 5 kHz). The stimulating electrode was purchased from WPI (WPI, TST33C05KT) and current was generated from a stimulus isolator. The digitized tracings were acquired to a Dell PC with pClamp 9.8. To collect field recordings, we first examined the fEPSP response to different stimulating current amplitudes to obtain an input–output curve. The fEPSP response was recorded from stimulus steps from 0 to 60 μA at 10 μA intervals. We evaluated the recordings and selected a stimulus intensity that produced 50% of the maximum fEPSP response, and exhibited a symmetrical geometry related to the downward and upward slope of the fEPSP. The selected stimulus intensity was delivered to the slice every 15 s to collect ten minutes of basal synaptic activity followed by a theta burst stimulation at 100 Hz (5 sweeps of 4 pulses delivered every 10 msec.). Following theta burst stimulation, fEPSP response to the same baseline stimulus was recorded for one hour every 15 s.

2.14. Statistical analysis

Data from experimental replicate sets were quantitated using Prism (GraphPad). Means of the combined proportions or cell numbers were compared using the *Student's t-test* with the threshold for significance set at 0.05. For multiple comparisons, one-way ANOVA with Tukey *post hoc* was used and statistical significance was set at 0.05. For categorical analyses, the Fisher exact test was used and statistical significance was set at 0.05. Error bars represent standard error of the mean (s.e.m).

3. Results

3.1. α2-chimaerin is localized to dendrites and spines in the hippocampus

The Rac-GAP α2-chimaerin is essential for the proper guidance of corticospinal, oculomotor, spinal interneuron and spinal motor neuron axons (Beg et al., 2007; Iwasato et al., 2007; Shi et al., 2007; Wegmeyer et al., 2007; Miyake et al., 2008; Ferrario et al., 2012; Kao et al., 2015). To determine if α2-chimaerin plays a role in regulating the structural and functional plasticity of dendrites and spines, we transfected wild type (WT) mouse hippocampal neurons with soluble mCherry and low levels of EGFP-tagged::α2-chimaerin. We found that EGFP::α2-chimaerin was expressed throughout the neuron with robust expression in dendrites and spines (Fig. 1A). The subcellular localization of EGFP::α2-chimaerin to dendritic spines suggests the protein is expressed at synapses, which is supported by biochemical studies demonstrating that α2-chimaerin is a tightly associated core component of the post-synaptic density (PSD) (Shi et al., 2007). Next, we analyzed α2-chimaerin transcription within the hippocampus by utilizing a beta-galactosidase (β-gal)

reporter that is inserted into the α2-chimaerin gene-trap cassette (Fig. 1B) (Beg et al., 2007). We prepared coronal slices from α2-chimaerin gene-trap homozygote mice ($\alpha2^{gt/gt}$) to determine the temporal onset and perdurance of α2-chimaerin transcription in context to critical developmental windows of hippocampal neuronal connectivity. At P5 we observed dense β-gal staining throughout the pyramidal cell layers, but sparse expression within the dentate granule cell layer. At P15 through P60 β-gal expression was uniform throughout the pyramidal and granule cell layers (Fig. 1B). However, by P90, expression of α2-chimaerin was absent in the dentate gyrus, whereas CA3-CA1 pyramidal cell expression remained robust. These data suggest that α2-chimaerin expression is differentially regulated in hippocampal subregions and may play a role in regulating dendrites and spines.

3.2. α2-chimaerin is a major negative regulator of Rac1 in the hippocampus

Several groups including ours have used recombinant expression systems to assay the Rac-GAP activity of α2-chimaerin. Given α2-chimaerin's spatial and temporal expression in the hippocampus, we sought to investigate if its loss altered active Rac1-GTP levels in mature hippocampal neurons. Primary hippocampal neurons cultured for 18–20 days in vitro (DIV) were lysed and a quantitative spectrophotometric assay was used to detect the cellular levels of active Rac1-GTP. Under basal conditions, α2-chimaerin mutant neurons had significantly increased active Rac1-GTP levels compared to controls, suggesting that α2-chimaerin is a major negative regulator of Rac1 in hippocampal neurons (Fig. 2A). In dendrites and spines, active Rac1 can promote F-actin polymerization by initiating downstream effector signaling pathways (Nakayama et al., 2000). Thus, we investigated if the heightened Rac1-GTP levels led to changes in polymerized F-actin in dendrites and spines. Primary hippocampal neurons were fixed and stained with fluorescently-tagged phalloidin, which binds selectivity to polymerized F-actin (Fig. 2B). Quantification revealed a significant increase in F-actin spine area and intensity selectively in dendritic spine heads, but not in the dendritic shaft in α2-chimaerin mutants (Fig. 2C).

3.3. α2-chimaerin regulates dendritic arborization and spine morphogenesis

To examine the role of α2-chimaerin in dendritic arborization and spine morphogenesis, we cultured primary hippocampal neurons from WT and $\alpha2^{gt/gt}$ mutant animals and transfected the cells with a β-actin-EGFP plasmid to assess basal dendrite morphology. Morphological quantitation at 18 DIV revealed α2-chimaerin mutant neurons exhibited a simplified basal dendritic arbor, and an overall reduction in total basal dendritic arbor length (Fig. 3A). To confirm our in vitro findings, we crossed $\alpha2^{gt/gt}$ mutants to Thy1-GFP-M animals, in which a sparse subset of CA1 pyramidal cells express GFP (Feng et al., 2000). Basal dendritic complexity and total dendritic length of CA1 pyramidal neurons was similarly simplified in $\alpha2^{gt/gt}$;GFP-M+ mutants as compared to GFP-M+ controls; thus, corroborating our in vitro findings and identifying α2-chimaerin as a key player in shaping dendritic arbor complexity (Fig. 3B).

Endogenous α2-chimaerin is a core component of the PSD (Iwasato et al., 2007; Shi et al., 2007) and EGFP::α2-chimaerin is localized throughout the dendritic 'spinoplasm' (Fig. 1A); thus, we investigated if loss of α2-chimaerin alters dendritic spine density and morphology. Loss of α2-chimaerin both in vitro and in vivo resulted in a significant decrease in the

number of protrusions emanating from secondary and tertiary dendritic shafts (Fig. 4A, B). To determine if specific classes of spines were affected by loss of α2-chimaerin, we quantitated spine shape frequency. Examples of our categorical classification of dendritic protrusions are shown (Fig. 4C): 1) filopodia: thin and narrow protrusions that lack a bulbous head; 2) stubby spines: a short bulbous head with an unresolved neck; 3) mushroom spines: a defined narrow neck terminating to a bulbous head; and 4) atypical spines: bifurcated where two spine heads share a common neck, or branched where secondary and tertiary spine heads branch from the primary spine head (Harris et al., 1992; Bourne and Harris, 2008). Quantification revealed the reduction in protrusion density was due to a selective loss of mushroom spines, whereas stubby spines and filopodia were unchanged compared to controls (Fig. 4D). Analysis of atypical spine types revealed a significant increase in irregular branched spines, but no change in bifurcated spines in α2-chimaerin mutants (Fig. 4D). Furthermore, loss of α2-chimaerin increased mushroom spine neck length and head area (Fig. 4E, F).

Given the significant presence of dysmorphic dendritic spine morphologies observed in several neurological diseases (Penzes et al., 2011), we next sought to determine if cell-autonomous neuronal loss of α2-chimaerin might also cause a similar increase in irregular branched spines observed in the constitutive gene-trap mutants. To this end, we generated three short hairpin RNAs (shRNAs) that specifically target murine α2-chimaerin (α2-sh1, α2-sh2, α2-sh3). First, we sh2, confirmed knockdown efficacy by co-transfecting HEK-293T cells with individual shRNAs plus a wild type HA-tagged-α2-chimaerin plasmid (HA::α2). Second, we confirmed the specificity of these shRNAs by generating an shRNA resistant HA::α2 plasmid in which the shRNA target sequence sites have been mutated. Third, we co-transfected an HA-tagged-α1-chimaerin plasmid (HA::α1) to determine if shRNA expression caused off-target effects that reduce α1-chimaerin protein levels. Whole cell western blot analyses revealed that the designed shRNAs showed high efficacy in reducing wild type α2-chimaerin protein levels compared to control scrambled shRNA (Fig. 5A). Co-transfection of shRNAs with the resistant HA::α2 plasmid did not alter protein levels compared to controls (Fig. 5A). Importantly, shRNA co-transfection with the wild type HA::α1 chimaerin plasmid did not show off target effects in reducing α1-chimaerin protein levels (Fig. 5A). The α2-sh2 target sequence showed the highest knockdown efficacy, thus we chose this construct for neuronal expression. We prepared lentiviral particles and infected WT primary hippocampal neurons to confirm that α2-sh2 could effectively reduce endogenous hippocampal neuron α2-chimaerin protein levels. Western blot analysis revealed that α2-sh2 infection strongly reduced endogenous α2-chimaerin protein in comparison to scramble infected controls (Fig. 5B).

To assess the effect of acute cell-autonomous α2-chimaerin suppression, wild type neurons were transfected with scramble or α2-sh2 plasmids at 10 DIV, and were fixed and analyzed at 16–18 DIV (Fig. 5C, D). Similar to the in vitro and in vivo findings, acute cell-autonomous knockdown resulted in a significant and selective loss of mushroom shaped spines, and an increase in atypical branched and bifurcated spines, when compared to scrambled control shRNA expressing neurons (Fig. 5D). Next, we demonstrated that the increased atypical branched spine density was specifically due to loss of α2-chimaerin, as re-expression of EGFP::α2-chimaerin at 10 DIV rescued the atypical dendritic spine defects.

(Fig. 5E, F). However, re-expression of EGFP::α2-chimaerin failed to rescue dendritic arborization complexity, suggesting that α2-chimaerin may serve different spatiotemporal roles in regulating Rac1 function during neuronal arbor and spine development (Fig 5G). Together, these data strongly argue that α2-chimaerin is a cell-autonomous and key regulator of mature spine morphologies.

3.4. α2-chimaerin regulates monosynaptic innervation

The hallmark of mature dendritic spines is that they form a single synapse with a presynaptic axon (Fiala et al., 2002). The selective loss of mature mushroom shaped spines coupled with increased atypical spines in α2-chimaerin mutants suggests that synaptic connectivity and function may be altered. To quantitate the density of possible synaptic contacts, 18 DIV hippocampal neurons were immunostained with the presynaptic marker synaptophysin (SYN) and the excitatory postsynaptic marker PSD-95 (Fig. 6A). In comparison to controls, α2-chimaerin mutants exhibited a significant increase in excitatory contacts along secondary and tertiary dendrites (Fig. 6B). To determine if the increased synaptic contacts were due to synaptic changes in specific spine classes, we counted the total number of synapses formed across dendritic segments and assigned each synapse to one of the categorical classes of spines described above. In control neurons, mushroom and stubby spines accounted for the majority of synapses (Fig. 6C). In α2-chimaerin mutants, mushroom-shaped spines also accounted for the majority of synapses, but atypical branched spines (21%) accounted for the second highest percentage of synapses, which was significantly increased compared to controls (6%) (Fig. 6C). Additionally, loss of α2-chimaerin resulted in an increased number of excitatory shaft synapses in comparison to controls (Fig. 6C). Thus, loss of α2-chimaerin not only shifts the distribution of synapse-to-spine type from mature mushroom synapses to atypical branched synapses, but also causes an increase in synaptic contacts per unit of dendrite length.

Atypical branched spines are rarely described in literature but their increased presence is a pathophysiological hallmark often observed in neurological disorders (Fiala et al., 2002; Penzes et al., 2011). Given that branched spines are detected more than two-fold in α2-chimaerin mutant neurons as compared to controls (Fig. 6E), we next assessed synaptic innervation on individual branched spines. We observed a significant difference in the innervated (mono + polysynaptic):non-innervated (no synaptic contact) ratio of branched spines between control (47:52%) and α2-chimaerin mutants (79:21%) (Fig. 6E). We determined mono- vs. polysynaptic innervation on branched spines as shown in Fig. 6D. Specifically, the branched spine on the left (a) exhibits one apposed SYN/PSD-95 synaptic contact and one SYN-negative, PSD-95 positive contact, thus it was categorized as monosynaptic (Fig. 6D). The branched spine on the right (b) exhibits two apposed SYN/PSD-95 synaptic contacts, and was categorized as polysynaptic (Fig. 6D). Non-synaptic branched spines exhibited no apposed SYN/PSD-95 contacts. In control neurons 52% of branched spines were non-synaptic, 25% were monosynaptic and 23% were polysynaptic. In contrast, α2-chimaerin mutant branched spines exhibited significant differences in that only 21% were non-synaptic, 32% were monosynaptic and 47% were polysynaptic (Fig. 6E). Together, these data suggest that atypical branched spine heads while structurally similar to single mature spines are capable of receiving multiple synaptic inputs.

3.5. α2-chimaerin is dispensable for CA3-CA1 long-term potentiation

The morphological and synaptic alterations in dendrites and spines suggest that α2-chimaerin may be a critical regulator of hippocampal network connectivity and function. A recent study reported that α2-chimaerin function is required during development to adjust cognitive ability in adulthood (Iwata et al., 2014, 2015). Specifically, loss of α2-chimaerin during early development was reported to increase contextual fear conditioning. Contextual fear conditioning relies on LTP-dependent mechanisms in the amygdala and hippocampus where circuits exhibit an increase in synaptic strength that presumably transmits information about the conditioned stimulus to neurons that have previously processed the neutral tone/context (Rogan et al., 1997; Stevens, 1998; Anagnostaras et al., 2001; Maren, 2001; Schafe et al., 2001). Our cellular findings of reduced dendritic complexity, decreased protrusion density, altered spine morphologies, and increased synaptic contacts suggest these key structural changes may account for the altered behavioral changes previously reported, as changes in spine number, morphology and plasticity are associated with LTP, which is an underlying cellular component of memory encoding and storage (Chen et al., 2007; Martinez and Tejada-Simon, 2011).

We assessed long-term potentiation in CA3-CA1 hippocampal synapses to assay the functional consequence of ablating α2-chimaerin. In brief, input–output curves revealed that the loss of α2-chimaerin resulted in no change between the presynaptic fiber volley and slope of the field excitatory postsynaptic potential (fEPSP), demonstrating that the basal transmission between CA3-CA1 hippocampal synapses was not modified as compared to controls (Fig. 7A). We next assessed synaptic plasticity by inducing LTP at Schaffer collateral afferents. Theta burst stimulation (100 Hz: 5 sweeps of 4 pulses every 10 msec.) of CA3 Schaffer collaterals revealed no difference in the induction or maintenance of LTP between CA3-CA1 hippocampal synapses in α2-chimaerin mutants as compared to controls (Fig. 7B). Taken together, these functional data demonstrate that CA3-CA1 hippocampal synaptic efficacy is neither compromised nor potentiated in α2-chimaerin mutants. However, the morphological and synaptic changes we identified may underlie defects or enhancements in other forms of synaptic signaling that mediate the cognitive defects previously reported in α2-chimaerin knockout mice (Iwata et al., 2014, 2015).

4. Discussion

The function of α2-chimaerin has been studied predominantly in the context of axonal guidance and locomotor circuit assembly (Beg et al., 2007; Iwasato et al., 2007; Wegmeyer et al., 2007; Miyake et al., 2008; Ferrario et al., 2012; Kao et al., 2015). Here, we identify a novel function for α2-chimaerin in regulating hippocampal neuron dendrite arborization and spine morphogenesis. Cellular, molecular and electro-physiological data reveal that loss of α2-chimaerin (1) simplifies dendritic arbor complexity, (2) decreases dendritic protrusion density, (3) induces atypical branched spine formation, (4) augments neuronal Rac1-GTP levels and increases spine head F-actin content, (5) increases the incidence of co-innervated atypical branched spines, but (6) is dispensable for hippocampal LTP. We discuss these findings in the context of the regulatory mechanisms of Rho-GTPase activity and the role of

actin-based structural and functional plasticity in neurological disorders associated with aberrant dendritic spine morphogenesis and plasticity.

The ability of dendritic spines to rapidly change shape is due to their highly enriched and labile F-actin cytoskeleton (Matus, 2000). As central regulators of actin cytoskeletal dynamics, the Rho-GTPases are critical determinants of spine morphogenesis and synaptic plasticity (Hall, 1998; Luo, 2000). The regulated cycling between active and inactive states is critically important as gain- and loss-of-function mutations in Rac1, RhoA and Cdc42 impact dendrite arborization and spine density, morphology and plasticity (Tolias et al., 2011). Furthermore, several disease-associated mutations have been identified in genes that regulate Rho-GTPase activity, underscoring that tight control of Rho-GTPase activity is imperative given their essential roles in diverse cellular processes (Penzes et al., 2011; Zoghbi and Bear, 2012). Although the molecular logic of GEF/GAP regulation of Rho-GTPases in response to synaptic activity is not well understood, the precise spatiotemporal activity of these modulatory proteins is likely to be highly choreographed and context-dependent (Duman et al., 2015). Thus, the cellular expression, subcellular localization, developmental regulation and protein-protein interactions of GEFs and GAPs are major factors that contribute to the spatiotemporal regulation and signaling specificity of Rho GTPases (Tolias et al., 2011).

4.1. Rac-GEF and Rac-GAP regulation of dendrites and spine morphogenesis

Several Rac-GEF proteins are known to localize at synapses and play critical roles in synaptogenesis (Tolias et al., 2005; Penzes and Jones, 2008). An emerging model is that Rac-GEFs play specific spatiotemporal roles in Rac1-dependent dendritic spine formation, maturation, maintenance and activity-dependent plasticity (Bai et al., 2015). For example, mice lacking the GEF Kalirin-7 exhibit decreased spine density and neurocognitive defects (Penzes et al., 2003). Kalirin-7 expression occurs later during development and is maintained throughout adulthood, suggesting that it's role may be important in spine maturation/maintenance as opposed to early synapse development (Xie et al., 2007; Ma et al., 2008; Cahill et al., 2009). Furthermore, RNAi knockdown of the Rac-GEF Tiam1 results in dendritic arbor simplification and a reduction in spine and synapse density (Tolias et al., 2005). Tiam1 interacts with the partitioning defective (PAR) protein PAR-3, which may act to spatially restrict Tiam1 to modulate a specific subpool of Rac1 within the dendritic spine head (Zhang and Macara, 2006; Tolias et al., 2011). While several other Rac-specific GEFs (i.e. α/β-PIX, Vav2/3, Farp1) are known to play important roles in dendrite arborization and spine morphogenesis, relatively few Rac-GAP proteins have been characterized whose loss of function affects dendrites and spines (i.e. BCR, ABR, srGAP, Rich2). The shorter α1-chimaerin isoform plays a role in the pruning of dendrites and spines, suggesting that as a family, the α-chimaerins are important regulators of neuronal arborization (Van de Ven et al., 2005; Buttery et al., 2006). We previously demonstrated that the mRNA and protein expression of the α1-chimaerin isoform are unaffected in the α2-chimaerin gene trap mutants (Beg et al., 2007). Importantly, our data demonstrate that dendritic dysmorphogenesis caused by loss of α2-chimaerin is not compensated for by α1-chimaerin, suggesting these two isoforms play unique and non-overlapping roles in dendritic arborization and spine morphogenesis.

Several studies involving manipulation of Rac1 function have provided the general consensus that increasing Rac1 activity leads to increased dendritic complexity, whereas decreasing Rac1 activity leads to dendritic simplification (Luo, 2000; Nakayama et al., 2000). Moreover, suppression of the Rac-GEFs Tiam1 and kalirin-7, which reduce active Rac1-GTP levels, have been shown to drive dendritic arbor simplification (Ma et al., 2003; Tolias et al., 2005). Paradoxically, our data demonstrates that loss of α2-chimaerin, which increases active Rac1-GTP, reduces dendritic complexity. Although surprising, our results are not without precedent as overexpression of constitutively active Rac1 has been previously shown to drive dendritic simplification in cerebellar Purkinje neurons (Luo et al., 1996). These data highlight the possibility that specific GEFs and GAPs may differentially modulate distinct pools of Rac1 to regulate dendritic growth and maintenance. Supporting this model, re-expression of EGFP::α2-chimaein was sufficient to rescue aberrant spine morphologies, but insufficient to rescue dendritic arbor complexity. We, and others have previously demonstrated that both α2-chimaerin gain and loss of function can yield similar defects in axonal guidance (Beg et al., 2007; Iwasato et al., 2007; Wegmeyer et al., 2007; Miyake et al., 2008; Clark et al., 2013; Kao et al., 2015). These data suggest that restricted pools or levels of activated α2-chimaerin may be critically important for the precise spatiotemporal regulation of Rac1 in dendrites and spines. These data highlight that Rac-GEF/GAP protein localization, developmental regulation, and protein-protein interactions are likely to be critical determinants in modulating the spatiotemporal activity of Rac1 in dendrites and spines.

4.2. Cell surface regulation of GEF and GAPs in dendrites and spines

Activity-dependent signal transduction pathways need to be tightly controlled to ensure that individual dendritic spines respond appropriately to local signals. Coupling upstream receptor activation to the correct downstream effector proteins permits signaling specificity and is essential for driving morphological and functional plasticity in activated spines. In this context, α2-chimaerin is known to interact with several receptor tyrosine kinase receptors that have important roles in dendritic spine morphogenesis and synaptic plasticity. Notably, the cell surface Eph receptors (EphRs) play essential roles in dendritic spine morphogenesis (Klein, 2004). Activation of EphA4 causes spine retraction and shortening, whereas EphB2 promotes spine formation, maintenance and clustering of NMDA receptors (Dalva et al., 2000; Zhou et al., 2012). An outstanding question is whether EphA4 and EphB1/2 receptors share common molecular pathways in differentially sculpting spines, or if they use distinct molecular pathways. Mounting evidence suggests that EphRs regulate spine morphogenesis and synaptic plasticity by modulating Rho-GTPase activity. Significantly, the Rac-GEFs Kalirin-7, Tiam1 and Intersectin-L are required for EphB-induced spine remodeling (Tolias et al., 2011). We have previously shown that α2-chimaerin interacts with both EphA4 and EphB1/2 receptors (Beg et al., 2007; Kao et al., 2015), and that loss of α2-chimaerin results in significant spine abnormalities. Together, these data suggest that the Rac-GAP α2-chimaerin may be a critical mediator of EphR-dependent spine morphogenesis and synaptic plasticity. However, it remains unclear what role α2-chimaerin plays in EphR-dependent spine morphogenesis. Is α2-chimaerin: 1) a dedicated EphA4 effector required for spine pruning; 2) required for EphB-mediated spine maturation and maintenance; or 3) a global EphR effector in spine morphogenesis? Given the paucity of Rac-GAP proteins that have

been characterized in spine morphogenesis, one possibility is that α2-chimaerin is recruited to synapses in response to EphR activation to counterbalance GEF activation of Rac1. Intriguingly, the similar dysmorphic spine phenotypes shared between EphA4 and α2-chimaerin mutant mice suggest that α2-chimaerin may be a critical downstream mediator of EphA4-dependent spine morphogenesis, which remains to be determined. Moreover, α2-chimaerin can biochemically interact with EphB1/2, but we have yet to identify a phenotype linked to these signaling pathways resulting from loss of α2-chimaerin (Kao et al., 2015). Adding to the complexity of GEF/GAP regulation, a recent and elegant study revealed that GEFs and GAPs can form regulatory complexes that modulate spine morphogenesis and synaptic plasticity (Um et al., 2014). Specifically, in response to BDNF-TrkB signaling, a GEF/GAP complex comprised of Tiam1 and BCR has been shown to dynamically regulate the spatiotemporal activity of Rac1 within spines. This intriguing example suggests that α2-chimaerin may form a similar regulatory complex with other GEF proteins to dynamically regulate spine morphogenesis and synaptic plasticity, but experimental evidence supporting this model remains to be determined.

4.3. Why is hippocampal LTP unaffected in α2-chimaerin mutants?

Actin cytoskeletal reorganization is critical for synaptic plasticity such as LTP (Chen et al., 2007). Disruption of other Rac-GAPs such as BCR, ABR and Rich2 result in decreased LTP maintenance, thus it is surprising that the loss of α2-chimaerin, which increases neuronal active Rac1-GTP and spine head F-actin, had no effect on LTP induction or maintenance (Oh et al., 2010). One possible model is that α2-chimaerin may function to maintain the mature morphological hallmarks of dendritic spines, but may not be critical for functional changes within the spine. Accordingly, it has been reported that different pools of F-actin within the spine serve distinct functions in hippocampal LTP induction and maintenance (Honkura et al., 2008). Moreover, distinct molecular pathways can modulate Rho-GTPase signaling in spines, which are required for either the induction or maintenance phases of LTP (Kennedy et al., 2005; Martinez and Tejada-Simon, 2011). An important observation from our results is that the structural abnormalities in the dendritic receptive field and at the single spine level are not reflected as functional deficits within the hippocampus. A possible explanation is that the high basal levels of active Rac1 caused by loss of α2-chimaerin may invoke compensatory mechanisms that homeostatically inhibit downstream pathways associated with LTP in CA3-CA1 hippocampal synapses. Alternatively, upregulation or enhanced activity of other Rac-GAPs such as BCR and ABR, or reduced activity of Rac-GEFs may compensate for loss of α2-chimaerin.

Mature mushroom spines are autonomous units that compartmentalize synaptic activity and restrict the diffusion of postsynaptic signaling molecules (Dailey and Smith, 1996; Harris, 1999). One possibility is that the dysmorphic spines in α2-chimaerin mutants may permit the spread of activity from one synapse to another, thereby compensating for alterations at the neuronal level to balance network activity. Alternatively, the increased occurrence of polysynaptic contacts on branched spines may compensate for the reduced protrusion density and simplified dendritic arbor. Although α2-chimaerin loss results in decreased protrusion density, the number of synaptic contacts per unit length is increased, which may

be a compensatory mechanism that equalizes synaptic drive in α2-chimaerin mutant neurons.

In conclusion, our study provides evidence that α2-chimaerin is a critical regulator of Rac1 activity in hippocampal neurons. Elucidating the detailed molecular mechanisms of how α2-chimaerin integrates and transduces cell-surface receptor activation to downstream effector pathways that alter dendritic spine cytoskeletal regulation are key questions for future studies.

Acknowledgments

We thank members of the Beg and Murphy laboratories for comments on the manuscript. We thank Georgina Nicholl for mouse colony maintenance, expert technical assistance, and critical feedback on the manuscript. We thank Yevgeniya Mironova and Roman Giger for preliminary electrophysiology data. We thank Dr. Peter Scheiffele for generously providing the α2-chimaerin gene trap mutant mice. This work was supported by the Alfred P. Sloan Foundation (FG-BR-5098), The Hartwell Foundation, a Basil O'Connor Starter Scholar Research Award, and the National Institute of Neurological Disorders and Stroke (R01NS094678-01A1) (A.A.B), a National Science Foundation Graduate Research Fellowship (DGE1256260) and University of Michigan Rackham Merit Fellowship (C.M.V.).

References

Anagnostaras SG, Gale GD, Fanselow MS. Hippocampus and contextual fear conditioning: recent controversies and advances. Hippocampus. 2001; 11:8–17. [PubMed: 11261775]

Bai Y, Xiang X, Liang C, Shi L. Regulating Rac in the nervous system: molecular function and disease implication of Rac GEFs and GAPs. Biomed Res Int. 2015; 2015:632450. [PubMed: 25879033]

Beg AA, Sommer JE, Martin JH, Scheiffele P. alpha2-chimaerin is an essential EphA4 effector in the assembly of neuronal locomotor circuits. Neuron. 2007; 55:768–778. [PubMed: 17785183]

Bhatt DH, Zhang S, Gan WB. Dendritic spine dynamics. Annu Rev Physiol. 2009; 71:261–282. [PubMed: 19575680]

Bos JL, Rehmann H, Wittinghofer A. GEFs and GAPs: critical elements in the control of small G proteins. Cell. 2007; 129:865–877. [PubMed: 17540168]

Bourne JN, Harris KM. Balancing structure and function at hippocampal dendritic spines. Annu Rev Neurosci. 2008; 31:47–67. [PubMed: 18284372]

Buttery P, Beg AA, Chih B, Broder A, Mason CA, Scheiffele P. The diacylglycerol-binding protein alpha1-chimaerin regulates dendritic morphology. Proc Natl Acad Sci USA. 2006; 103:1924–1929. [PubMed: 16446429]

Cahill ME, Xie Z, Day M, Photowala H, Barbolina MV, Miller CA, Weiss C, Radulovic J, Sweatt JD, Disterhoft JF, Surmeier DJ, Penzes P. Kalirin regulates cortical spine morphogenesis and disease-related behavioral phenotypes. Proc Natl Acad Sci USA. 2009; 106:13058–13063. [PubMed: 19625617]

Chen LY, Rex CS, Casale MS, Gall CM, Lynch G. Changes in synaptic morphology accompany actin signaling during LTP. J Neurosci. 2007; 27:5363–5372. [PubMed: 17507558]

Cherfils J, Zeghouf M. Regulation of small GTPases by GEFs, GAPs, and GDIs. Physiol Rev. 2013; 93:269–309. [PubMed: 23303910]

Clark C, Austen O, Poparic I, Guthrie S. alpha2-Chimaerin regulates a key axon guidance transition during development of the oculomotor projection. J Neurosci. 2013; 33:16540–16551. [PubMed: 24133258]

Dailey ME, Smith SJ. The dynamics of dendritic structure in developing hippocampal slices. J Neurosci. 1996; 12:2983–2994. [PubMed: 8622128]

Dalva MB, Takasu MA, Lin MZ, Shamah SM, Hu L, Gale NW, Greenberg ME. EphB receptors interact with NMDA receptors and regulate excitatory synapse formation. Cell. 2000; 103:945–956. [PubMed: 11136979]

Dong JM, Smith P, Hall C, Lim L. Promoter region of the transcriptional unit for human α1-chimaerin, a neuron-specific GTPase-activating protein for p21rac. Eur J Biochem. 1995; 227:636–646. [PubMed: 7867622]

Duman JG, Mulherkar S, Tu YK, JXC, Tolias KF. Mechanisms for spatiotemporal regulation of Rho-GTPase signaling at synapses. Neurosci Lett. 2015; 601:4–10. [PubMed: 26003445]

Ellis BL, Potts PR, Porteus MH. Creating higher titer lentivirus with caffeine. Hum Gene Ther. 2011; 22:93–100. [PubMed: 20626321]

Feng G, Mellor RH, Bernstein M, Keller-Peck C, Nguyen QT, Wallace M, Nerbonne JM, Lichtman JW, Sanes JR. Imaging neuronal subsets in transgenic mice expressing multiple spectral variants of GFP. Neuron. 2000; 28:41–51. [PubMed: 11086982]

Ferrario JE, Baskaran P, Clark C, Hendry A, Lerner O, Hintze M, Allen J, Chilton JK, Guthrie S. Axon guidance in the developing ocular motor system and Duane retraction syndrome depends on Semaphorin signaling via alpha2-chimaerin. Proc Natl Acad Sci USA. 2012; 109:14669–14674. [PubMed: 22912401]

Fiala JC, Spacek J, Harris KM. Dendritic spine pathology: cause or consequence of neurological disorders? Brain Res Brain Res Rev. 2002; 39:29–54. [PubMed: 12086707]

Fischer M, Kaech S, Wagner U, Brinkhaus H, Matus A. Glutamate receptors regulate actin-based plasticity in dendritic spines. Nat Neurosci. 2000; 3:887–894. [PubMed: 10966619]

Goodman CS, Shatz CJ. Developmental mechanisms that generate precise patterns of neuronal connectivity. Cell. 1993; 72:77–98. [PubMed: 8428376]

Hall A. Rho GTPases and the actin cytoskeleton. Science. 1998; 279:509–514. [PubMed: 9438836]

Harris KM. Structure, development, and plasticity of dendritic spines. Curr Opin Neurobiol. 1999; 9:343–348. [PubMed: 10395574]

Harris KM, FEJBT. Three-dimensional structure of dendritic spines and synapses in rat hippocampus (CAI) at postnatal day 15 and adult ages: implications for the maturation of synaptic physiology and long-term potentiation. J Neurosci. 1992; 12:2685–2705. [PubMed: 1613552]

Hausser M, Spruston N, Stuart GJ. Diversity and dynamics of dendritic signaling. Science. 2000; 290:739–744. [PubMed: 11052929]

Honkura N, Matsuzaki M, Noguchi J, Ellis-Davies GC, Kasai H. The subspine organization of actin fibers regulates the structure and plasticity of dendritic spines. Neuron. 2008; 57:719–729. [PubMed: 18341992]

Iwasato T, Katoh H, Nishimaru H, Ishikawa Y, Inoue H, Saito YM, Ando R, Iwama M, Takahashi R, Negishi M. Rac-GAP α-chimerin regulates motor-circuit formation as a key mediator of EphrinB3/EphA4 forward signaling. Cell. 2007; 130:742–753. [PubMed: 17719550]

Iwata R, Matsukawa H, Yasuda K, Mizuno H, Itohara S, Iwasato T. Developmental RacGAP alpha2-chimaerin signaling is a determinant of the morphological features of dendritic spines in adulthood. J Neurosci. 2015; 35:13728–13744. [PubMed: 26446225]

Iwata R, Ohi K, Kobayashi Y, Masuda A, Iwama M, Yasuda Y, Yamamori H, Tanaka M, Hashimoto R, Itohara S, Iwasato T. RacGAP α2-chimaerin function in development adjusts cognitive ability in adulthood. Cell Rep. 2014; 8:1257–1264. [PubMed: 25159148]

Kaech S, Banker G. Culturing hippocampal neurons. Nat Protoc. 2006; 1:2406–2415. [PubMed: 17406484]

Kao TJ, Nicholl GC, Johansen JA, Kania A, Beg AA. alpha2-chimaerin is required for Eph receptor-class-specific spinal motor axon guidance and coordinate activation of antagonistic muscles. J Neurosci. 2015; 35:2344–2357. [PubMed: 25673830]

Kennedy MB, Beale HC, Carlisle HJ, Washburn LR. Integration of biochemical signalling in spines. Nat Rev Neurosci. 2005; 6:423–434. [PubMed: 15928715]

Klein R. Eph/ephrin signaling in morphogenesis, neural development and plasticity. Curr Opin Cell Biol. 2004; 16:580–589. [PubMed: 15363810]

Longair MH, Baker DA, Armstrong JD. Simple Neurite Tracer: open source software for reconstruction, visualization and analysis of neuronal processes. Bioinformatics. 2011; 27:2453–2454. [PubMed: 21727141]

Luo L. Rho GTPases in neuronal morphogenesis. Nat Rev Neurosci. 2000; 1:173–180. [PubMed: 11257905]

Luo L, Hensch TK, Ackerman L, Barbel S, Jan LY, Jan YN. Differential effects of the Rac GTPase on Purkinje cell axons and dendritic trunks and spines. Nature. 1996; 379:837–840. [PubMed: 8587609]

Ma XM, Huang J, Wang Y, Eipper BA, Mains RE. Kalirin, a multifunctional Rho guanine nucleotide exchange factor, is necessary for maintenance of hippocampal pyramidal neuron dendrites and dendritic spines. J Neurosci. 2003; 23:10593–10603. [PubMed: 14627644]

Ma XM, Kiraly DD, Gaier ED, Wang Y, Kim EJ, Levine ES, Eipper BA, Mains RE. Kalirin-7 is required for synaptic structure and function. J Neurosci. 2008; 28:12368–12382. [PubMed: 19020030]

Maren S. Neurobiology of Pavlovian fear conditioning. Annu Rev Neurosci. 2001; 24:897–931. [PubMed: 11520922]

Martinez LA, Tejada-Simon MV. Pharmacological inactivation of the small GTPase Rac1 impairs long-term plasticity in the mouse hippocampus. Neuropharmacology. 2011; 61:305–312. [PubMed: 21569781]

Matus A. Actin-based plasticity in dendritic spines. Science. 2000; 290:754–758. [PubMed: 11052932]

Meijering E. Neuron tracing in perspective. Cytometry A. 2010; 77A:693–704. [PubMed: 20583273]

Miyake N, Chilton J, Psatha M, Cheng L, Andrews C, Chan W-M, Law K, Crosier M, Lindsay S, Cheung M. Human CHN1 mutations hyperactivate α2-chimaerin and cause Duane's retraction syndrome. Science. 2008; 321:839–843. [PubMed: 18653847]

Nakayama AY, Harms MB, Luo L. Small GTPases Rac and Rho in the maintenance of dendritic spines and branches in hippocampal pyramidal neurons. J Neurosci. 2000; 20:5329–5338. [PubMed: 10884317]

Oh D, et al. Regulation of synaptic Rac1 activity, long-term potentiation maintenance, and learning and memory by BCR and ABR Rac GTPase-activating proteins. J Neurosci. 2010; 30:14134–14144. [PubMed: 20962234]

Penzes P, Jones KA. Dendritic spine dynamics—a key role for kalirin-7. Trends Neurosci. 2008; 31:419–427. [PubMed: 18597863]

Penzes P, Cahill ME, Jones KA, VanLeeuwen JE, Woolfrey KM. Dendritic spine pathology in neuropsychiatric disorders. Nat Neurosci. 2011; 14:285–293. [PubMed: 21346746]

Penzes P, Beeser A, Chernoff J, Schiller MR, Eipper BA, Mains RE, Huganir RL. Rapid induction of dendritic spine morphogenesis by trans-synaptic ephrinB-EphB receptor activation of the Rho-GEF kalirin. Neuron. 2003; 37:263–274. [PubMed: 12546821]

Rogan MT, Staubli UV, LeDoux JE. Fear conditioning induces associative long-term potentiation in the amygdala. Nature. 1997; 390:604–607. [PubMed: 9403688]

Schafe GE, Nader K, Blair HT, LeDoux JE. Memory consolidation of Pavlovian fear conditioning: a cellular and molecular perspective. Trends Neurosci. 2001; 24:540–546. [PubMed: 11506888]

Segal M, Andersen P. Dendritic spines shaped by synaptic activity. Curr Opin Neurobiol. 2000; 10:582–586. [PubMed: 11084320]

Shi L, Fu WY, Hung KW, Porchetta C, Hall C, Fu AK, Ip NY. Alpha2-chimaerin interacts with EphA4 and regulates EphA4-dependent growth cone collapse. Proc Natl Acad Sci USA. 2007; 104:16347–16352. [PubMed: 17911252]

Srivastava DP, Woolfrey KM, Penzes P. Analysis of dendritic spine morphology in cultured CNS neurons. J Vis Exp. 2011:e2794. [PubMed: 21775964]

Stevens CF. A million dollar question: does LTP = memory? Neuron. 1998; 20:1–2. [PubMed: 9459434]

Tolias KF, Duman JG, Um K. Control of synapse development and plasticity by Rho GTPase regulatory proteins. Prog Neurobiol. 2011; 94:133–148. [PubMed: 21530608]

Tolias KF, Bikoff JB, Burette A, Paradis S, Harrar D, Tavazoie S, Weinberg RJ, Greenberg ME. The Rac1-GEF Tiam1 couples the NMDA receptor to the activity-dependent development of dendritic arbors and spines. Neuron. 2005; 45:525–538. [PubMed: 15721239]

Um K, Niu S, Duman JG, Cheng JX, Tu Y-K, Schwechter B, Liu F, Hiles L, Narayanan AS, Ash RT. Dynamic control of excitatory synapse development by a Rac1 GEF/GAP regulatory complex. Dev Cell. 2014; 29:701–715. [PubMed: 24960694]

Van de Ven TJ, VanDongen HM, VanDongen AM. The nonkinase phorbol ester receptor alpha 1-chimerin binds the NMDA receptor NR2A subunit and regulates dendritic spine density. J Neurosci. 2005; 25:9488–9496. [PubMed: 16221859]

Wegmeyer H, Egea J, Rabe N, Gezelius H, Filosa A, Enjin A, Varoqueaux F, Deininger K, Schnütgen F, Brose N. EphA4-dependent axon guidance is mediated by the RacGAP α2-chimaerin. Neuron. 2007; 55:756–767. [PubMed: 17785182]

Xie Z, Srivastava DP, Photowala H, Kai L, Cahill ME, Woolfrey KM, Shum CY, Surmeier DJ, Penzes P. Kalirin-7 controls activity-dependent structural and functional plasticity of dendritic spines. Neuron. 2007; 56:640–656. [PubMed: 18031682]

Zhang H, Macara IG. The polarity protein PAR-3 and TIAM1 cooperate in dendritic spine morphogenesis. Nat Cell Biol. 2006; 8:227–237. [PubMed: 16474385]

Zhou L, Jones EV, Murai KK. EphA signaling promotes actin-based dendritic spine remodeling through slingshot phosphatase. J Biol Chem. 2012; 287:9346–9359. [PubMed: 22282498]

Zoghbi HY, Bear MF. Synaptic dysfunction in neurodevelopmental disorders associated with autism and intellectual disabilities. Cold Spring Harb Perspect Biol. 2012:4.

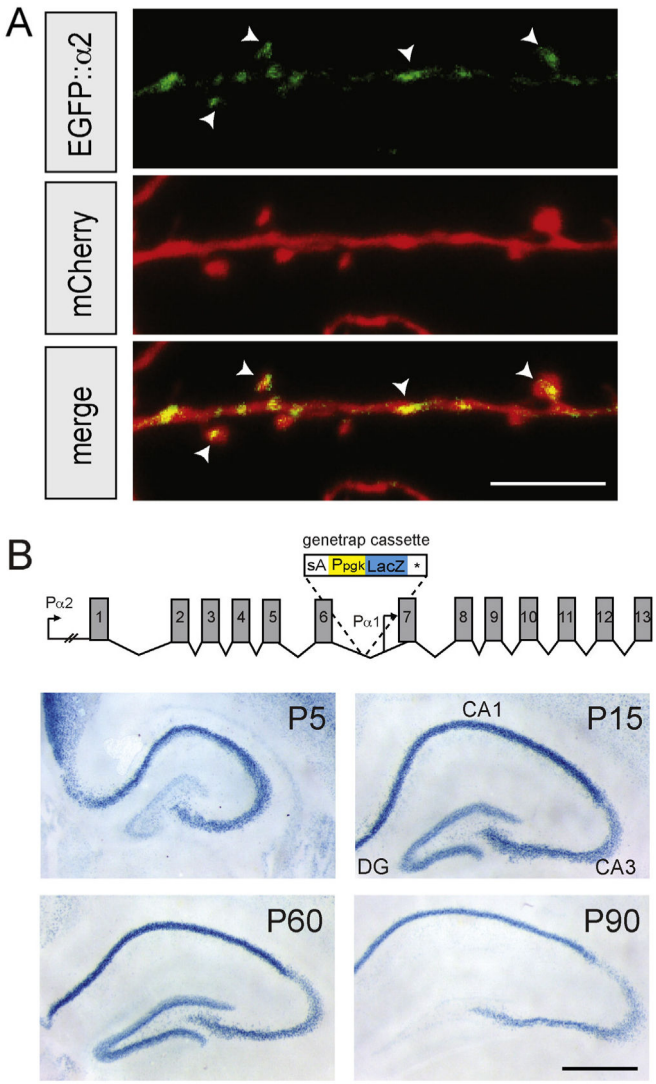

Fig. 1.

Alpha2-chimaerin is localized to hippocampal dendrites and is developmentally regulated in the hippocampus. (A) Wild-type primary hippocampal neurons were co-transfected at 16 DIV with 50 ng of EGFP::α2-chimaerin and 550 ng of mCherry to resolve fine dendritic structures. EGFP-α2-chimaerin is expressed throughout the spine head cytoplasm, but appears more punctate in the dendritic shaft. Scale bar equals 5 μm. (B) *Top*, schematic of the *CHN1* genomic locus. The genetrap cassette is inserted between exons 6–7. Placement of the genetrap cassette is upstream of the minimal α1-chimaerin promoter (Dong et al., 1995). The genetrap cassette consists of a splice acceptor (sA), a PGK promoter (Ppgk) driving β-galactosidase (lacZ), followed by a termination sequence. *Bottom*, representative images of coronal slices from α2-chimaerin genetrap homozygous animals at various timepoints. Transcriptional lacZ reporter expression reveals α2-chimaerin is expressed throughout the hippocampus during development. Dentate gyrus (DG) expression is absent at P90, while CA3 and CA1 expression remains. Scale bar is 200 μm.

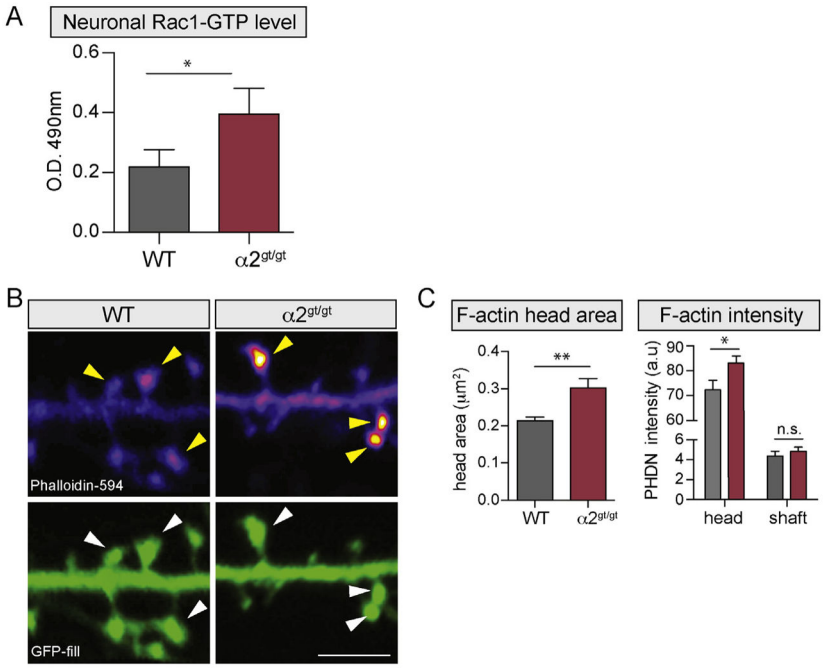

Fig. 2.

Alpha2-chimaerin is a major negative regulator of Rac1 and F-actin levels in hippocampal neurons. (A) Quantitative Rac1-GTP assay from WT and $\alpha2^{gt/gt}$ mutant primary hippocampal neuronal lysates (18–20 DIV). Optical density (OD490) measurements of Rac1-GTP (mean ± SEM): WT = 0.218 ± 0.134 vs. $\alpha2^{gt/gt}$ = 0.395 ± 0.148; *p = 0.0331. N = 4 experimental sets per genotype (2 dishes/experimental set); paired two-tailed *t-test*, α = 0.05. (B) Representative dendritic segments from WT and $\alpha2^{gt/gt}$ mutant hippocampal neurons at 18 DIV. Neurons were transfected with GFP to resolve fine dendritic structures, and treated with Alexa594-phalloidin to label polymerized F-actin. The white arrowheads mark GFP-filled dendritic spines, and the yellow arrowhead delineate polymerized F-actin in these same dendritic spines. Phalloidin intensity is shown as a pseudo-colored heat map, warmer colors are higher intensity. Scale bar is 5 μm. (C) *Left*, quantification of dendritic F-actin spine head area (μm^2) (mean ± SEM): WT = 0.224 ± 0.012 (n = 112) vs. $\alpha2^{gt/gt}$ = 0.308 ± 0.019 (n = 108), **p < 0.0001. *Right*, Quantification of phalloidin fluorescence intensity (a.u.) in the spine head (mean ± SEM): WT = 74.03 ± 3.0 (n = 112) vs. $\alpha2^{gt/gt}$ = 83.17 ± 3.38 (n = 108), *p = 0.0444. Quantification of phalloidin intensity in the dendritic shaft (mean ± SEM): WT = 4.434 ± 0.360 (n = 112) vs. $\alpha2^{gt/gt}$ = 4.863 ± 0.382 (n = 108), p = 0.4165, not significant (n.s.). WT: N = 3 experimental sets, 10 cells; and $\alpha2^{gt/gt}$: N = 3 experimental sets, 11 cells. (n = total # spines analyzed). Unpaired two-tailed Student *t-test*, α = 0.05.

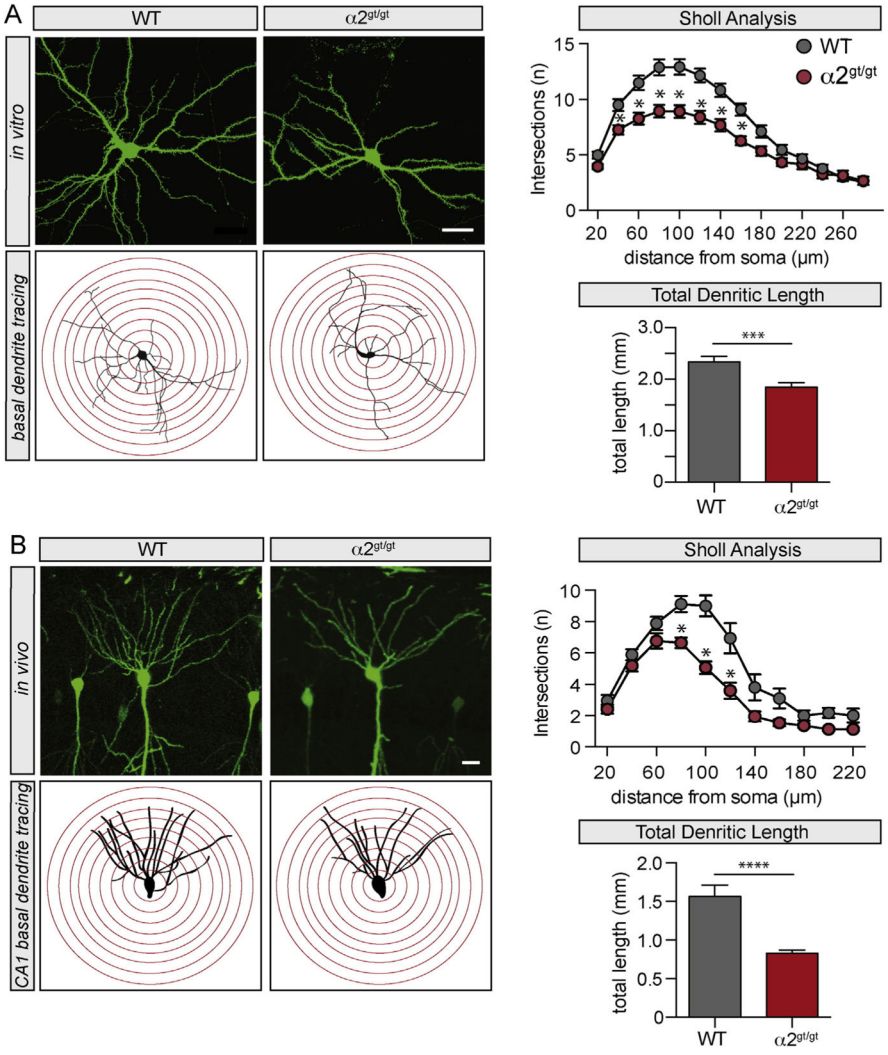

Fig. 3.

Loss of alpha2-chimaerin simplifies hippocampal dendritic arborization. (A) *Left*, (top) in vitro, representative images of WT and $\alpha2^{gt/gt}$ mutant primary hippocampal neurons at 16 DIV. *Left*, (below), representative skeleton outline tracings of basal dendrites from in vitro *cultured neurons*. Concentric circles (20 μm) are shown in red. *Right*, (top) Sholl analysis of hippocampal dendrite arborization, reveals α2-chimaerin mutant neurons ($\alpha2^{gt/gt}$) exhibit reduced basal dendritic complexity, N = 6 experimental sets/genotype; n = 75 cells/genotype, *t-test*, *Holm-Sidak*, $\alpha = 0.05$, $^{*}p < 0.001$. *Right*, (below), total basal dendritic length is significantly reduced in α2-chimaerin mutant neurons ($\alpha2^{gt/gt}$) compared to controls, N = 6 experimental sets/genotype; n = 75 cells/genotype, *unpaired t-test*, $\alpha = 0.05$, $^{***}p = 0.0005$. Scale bar equals 30 μm. (*B*) *Left*, (top) in vivo, representative images of CA1 basal dendrites from WT;Thy1-GFP-M+ and $\alpha2^{gt/gt}$;Thy1-GFP-M+ hippocampal slices. *Left*, (below), representative skeleton outline tracings from in vivo slices of CA1 basal dendrite arbor complexity. Concentric circles (20 μm) are shown in red. *Right*, (top) Sholl analysis of hippocampal dendrite arborization in vivo reveals α2-chimaerin mutant neurons ($\alpha2^{gt/gt}$) exhibit reduced basal dendritic complexity, N = 3 experimental sets/genotype; n =

17 cells/genotype, *t-test*, *Holm-Sidak*, $\alpha = 0.05$, $^{*}p < 0.004$. *Right*, (below), total basal dendritic length is significantly reduced in α2-chimaerin mutant neurons ($\alpha2^{gt/gt}$) compared to controls, N = 3 experimental sets/genotype; n = 17 cells/genotype, *unpaired t-test*, $\alpha = 0.05$, $^{****}p < 0.0001$. Scale bar equals 30 μm.

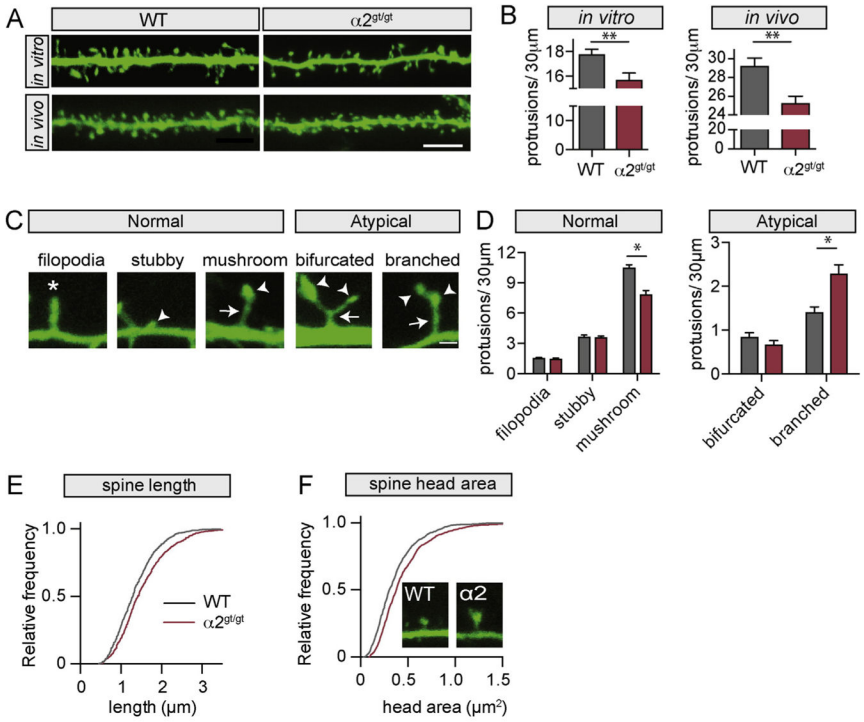

Fig. 4.

Alpha2-chimaerin is a key regulator of mature spine morphology. (A) In vitro and in vivo representative images of WT and $\alpha2^{gt/gt}$ mutant hippocampal dendritic segment. Scale bar equals 5 μm. (B) $\alpha2^{gt/gt}$ mutant dendrites exhibit reduced protrusion density. *Left*, in vitro quantification of dendritic protrusion density (mean ± SEM/30 μm): WT = 17.71 ± 0.46 (n = 1753) vs. $\alpha2^{gt/gt}$ = 15.66 ± 0.58 (n = 1566), $^{**}p = 0.0068$. *Right*, in vivo quantification of CA1 basal dendritic protrusion density: WT = 29.17 ± 0.91 (n = 1050) vs. $\alpha2^{gt/gt}$ = 25.17 ± 0.84, (n = 906), $^{**}p = 0.0019$. In vitro quantification, WT: N = 6 experimental sets, 33 cells, 100 segments (30 μm), and $\alpha2^{gt/gt}$: N = 6 experimental sets, 32 cells, 100 segments (30 μm). In vivo quantification, WT: N = 3 experimental sets, 8 cells, 32 segments (30 μm), and $\alpha2^{gt/gt}$: N = 3 experimental sets, 7 cells, 32 segments (30 μm). Statistical significance determined using unpaired two-tailed Student *t-test*, $\alpha = 0.05$. (n = total # protrusions analyzed). (C) Dendritic spines were categorized based on their morphological structures. Filopodia protrusions lack a bulbous head (white asterisk); stubby protrusions lack a spine neck, while mushroom, branched and bifurcated spines exhibit a spine neck (white arrow) and spine head(s) (white arrowhead). Scale bar equals 1 μm. (D) $\alpha2^{gt/gt}$ mutant hippocampal neurons exhibit a reduction in mushroom spine density, in vitro. *Left*, Normal protrusion shape density quantification (mean ± SEM/30 μm): *filopodia*: WT = 1.46 ± 0.121 (n = 145) vs. $\alpha2^{gt/gt}$ = 1.42 ± 0.115 (n = 142), $p = 0.788$; *stubby*: WT = 3.59 ± 0.212 (n = 356) vs. $\alpha2^{gt/gt}$ = 3.53 ± 0.213 (n = 353), $p = 0.826$; *mushroom*: WT = 10.42 ± 0.365 (n = 1032) vs. $\alpha2^{gt/gt}$ = 7.77 ± 0.464 (n = 777), $^{*}p < 0.0001$. $\alpha2^{gt/gt}$ mutant hippocampal neurons exhibit an increase in atypical dendritic spines in vitro. *Right*, Atypical dendritic spine density quantification (mean ± SEM/30 μm) revealed a significant difference in branched spine density: WT = 1.39 ± 0.13 (n = 138) vs. $\alpha2^{gt/gt}$ = 2.28 ± 0.21 (n = 228), $^{*}p < 0.0001$, but no change in bifurcated spine density: WT = 0.82 ± 0.118 (n = 82) vs. $\alpha2^{gt/gt}$ = 0.66 ± 0.105 (n

= 66), $p = 0.289$. WT: N = 6 experimental sets, 33 cells, 100 segments (30 μm), and $\alpha 2^{gt/gt}$: N = 6 experimental sets, 32 cells, 100 segments (30 μm). Statistical significance determined using *t-test*, Holm-Sidak, $\alpha = 0.05$. (n = total # spines analyzed). (E) $\alpha 2^{gt/gt}$ mutant hippocampal neurons exhibit increased mushroom spine length. Cumulative frequency distribution of mushroom spine length (mean ± SEM): WT = 1.35 ± 0.017 (n = 819), N = 6 experimental sets, 32 cells vs. $\alpha 2^{gt/gt}$ = 1.54 ± 0.022 (n = 813), N = 6 experimental sets, n = 33 cells. Unpaired two-tailed *t-test*, $^{**}p < 0.0001$. (n = total # spines analyzed). (F) $\alpha 2^{gt/gt}$ mutant hippocampal neurons exhibit an increase in mushroom spine head area. Cumulative frequency distribution of mushroom spine head area (mean ± SEM): WT = 0.36 μm^2 ± 0.0081 (n = 819), N = 6 experimental sets, n = 32 cells vs. $\alpha 2^{gt/gt}$ = 0.45 μm^2 ± 0.0098 (n = 813), N = 6 experimental sets, n = 33 cells. Unpaired two-tailed *t-test*, $^{**}p < 0.0001$. Insert, representative images of WT and $\alpha 2^{gt/gt}$ mutant mushroom dendritic spines. (n = total # spines analyzed).

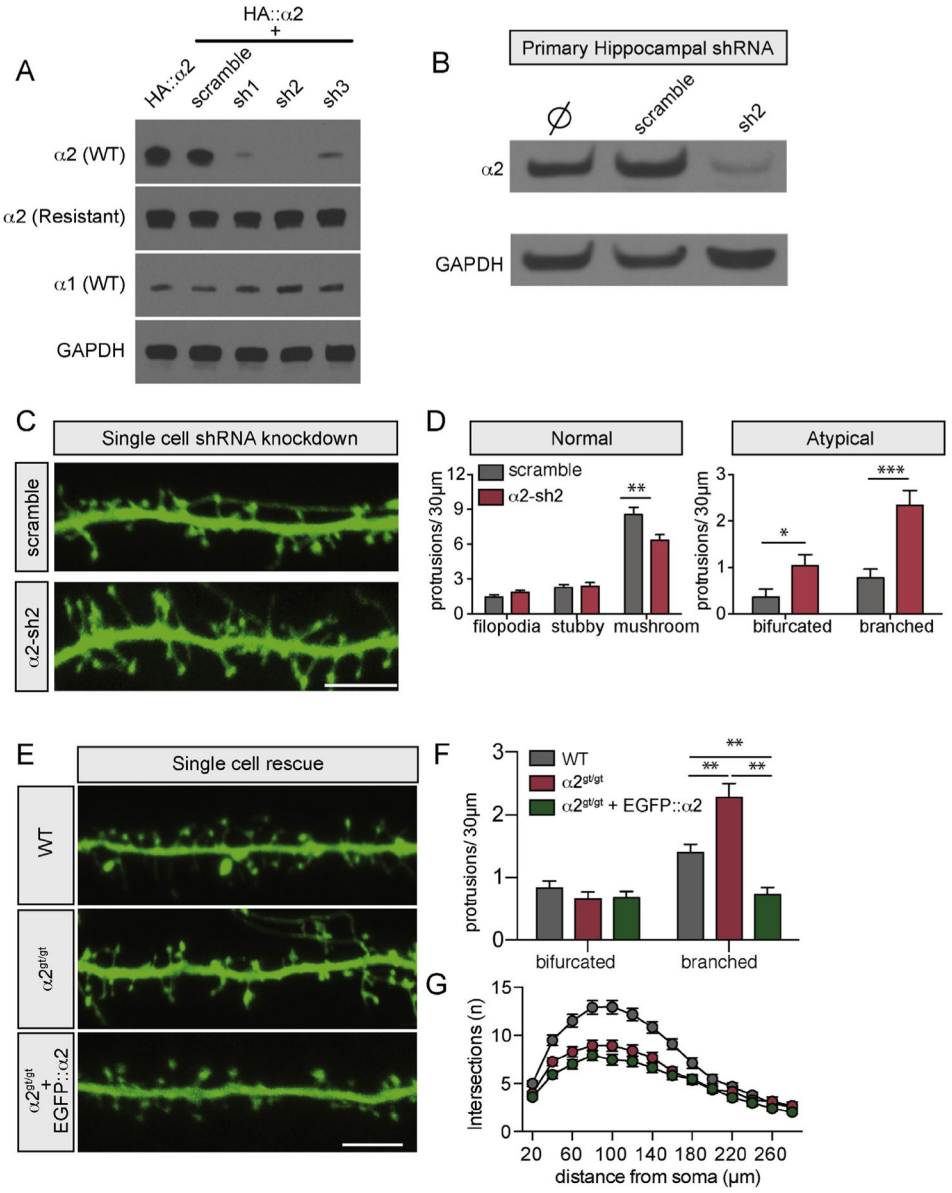

Fig. 5.

Alpha2-chimaerin is a cell-autonomous determinant of dendritic spine morphology. (A) Western blot of HEK-293T cell lysates transfected with wild type HA::α2, HA::α2 shRNA resistant, or wild type HA::α1 plasmids alone or co-transfected with scramble (control) or α2-chimaerin specific shRNAs (sh1, sh2, sh3). Cells were lysed 48 h after transfection, and whole cell lysates (10 μg) were probed with an *anti*-HA specific antibody and GAPDH as a loading control. The sh2 targeting construct was the most effective at reducing α2-chimaerin protein expression compared to scramble control. The shRNAs had no effect on protein expression when co-transfected with the HA::α2 shRNA resistant plasmid. Additionally, the shRNAs did not reduce HA::α1-chimaerin protein levels compared to control, demonstrating the efficacy and specificity of the designed shRNAs. (B) Western blot of primary hippocampal neuronal lysate infected with α2-sh2 or scramble control lentivirus at

5 DIV. Non-infected neuronal lysates are shown (∅). Infected neurons were lysed at 11 DIV, and whole cell lysates (20 μg) were probed with an *anti*-α2-chimaerin specific antibody and GAPDH as a loading control. α2-sh2 lentivirus is effective at reducing endogenous α2-chimaerin protein levels. (C) Representative images of 16 DIV dendritic segments from WT primary neurons transfected at 10 DIV with scramble or α2-chimaerin specific shRNAs (α2-sh2), respectively. Scale bar equals 5 μm. (D) *Left*, alpha2-chimaerin suppression did not affect the density of filopodia or stubby spines, but significantly decreased the density of mature mushroom shaped spines. Quantification of normal spine classes (mean ± SEM/30 μm): *filopodia*: scramble = 1.45 ± 0.194 (n = 32) vs. α2-sh2 = 1.85 ± 0.174 (n = 50), p = 0.135; *stubby*: scramble = 2.27 ± 0.272 (n = 50) vs. α2-sh2 = 2.41 ± 0.298 (n = 65), p = 0.745; *mushroom* = 8.54 ± 0.623 (n = 188) vs. α2-sh2 = 6.33 ± 0.506 (n = 171), $^{**}p$ = 0.007. *Right*, α2-chimaerin knockdown increases the density of atypical bifurcated and branched dendritic spines. Quantification of atypical dendritic spines (mean ± SEM/30 μm): *bifurcated*: scramble = 0.36 ± 0.168 (n = 8) vs. α2-sh2 = 1.037 ± 0.235 (n = 28), $^{*}p$ = 0.0307; *branched*: scramble = 0.77 ± 0.19 (n = 17) vs. α2-sh2 = 2.33 ± 0.320 (n = 63), $^{***}p$ = 0.0003. N = 3 experimental sets, 9 cells, 27 dendritic segments (30 μm) per condition. Significance was calculated using unpaired Student *t-test*, Holm-Sidak, α = 0.05. (n = total # spines analyzed). (E) Representative images of 16 DIV dendritic segments from WT primary neurons (top), $\alpha2^{gt/gt}$ mutant neurons (middle) transfected with GFP at 10 DIV. $\alpha2^{gt/gt}$ mutant neurons (bottom) re-expressing EGFP::α2-chimaerin. Scale bar equals 5 μm. (F) Exogenous re-expression of α2-chimaerin rescues atypical branched spine density in $\alpha2^{gt/gt}$ mutant hippocampal neurons. Quantification of atypical bifurcated spine density (mean ± SEM): WT = 0.828 ± 0.118 (n = 82) vs. $\alpha2^{gt/gt}$ = 0.66 ± 0.11 (n = 66) vs. $\alpha2^{gt/gt}$ + EGFP::α2 = 0.679 ± 0.0974 (n = 28), revealed no significant differences between experimental conditions, One-way ANOVA, *Tukey post-hoc*, $p \geq 0.05$. Quantification of atypical branched spine density (mean ± SEM): WT = 1.39 ± 0.137 (n = 138) vs. $\alpha2^{gt/gt}$ = 2.280 ± 0.22 (n = 228) vs. $\alpha2^{gt/gt}$ + EGFP::α2 = 0.73 ± 0.11 (n = 102), revealed a significant difference. One-way ANOVA, Tukey *post-hoc* $^{**}p < 0.001$. N = 6 experimental sets for all conditions; WT: n = 33 cells; $\alpha2^{gt/gt}$: n = 32 cells; $\alpha2^{gt/gt}$ + EGFP::α2: n = 25 cells. 80 dendritic segments (30 μm) were analyzed per condition. (n = total # spines analyzed). (G) Re-expression of EGFP::α2-chimaerin does not rescue dendritic complexity in vitro. Sholl analysis of hippocampal dendrite arborization. WT and $\alpha2^{gt/gt}$: N = 6 experimental sets/genotype, 75 cells/genotype. $\alpha2^{gt/gt}$ + EGFP::α2: N = 6 experimental sets/genotype, 45 cells. EGFP::α2-chimaerin re-expression failed to rescue the $\alpha2^{gt/gt}$ dendritic arborization defect in vitro. Student *t-test*, *Holm Sidak*, α = 0.05.

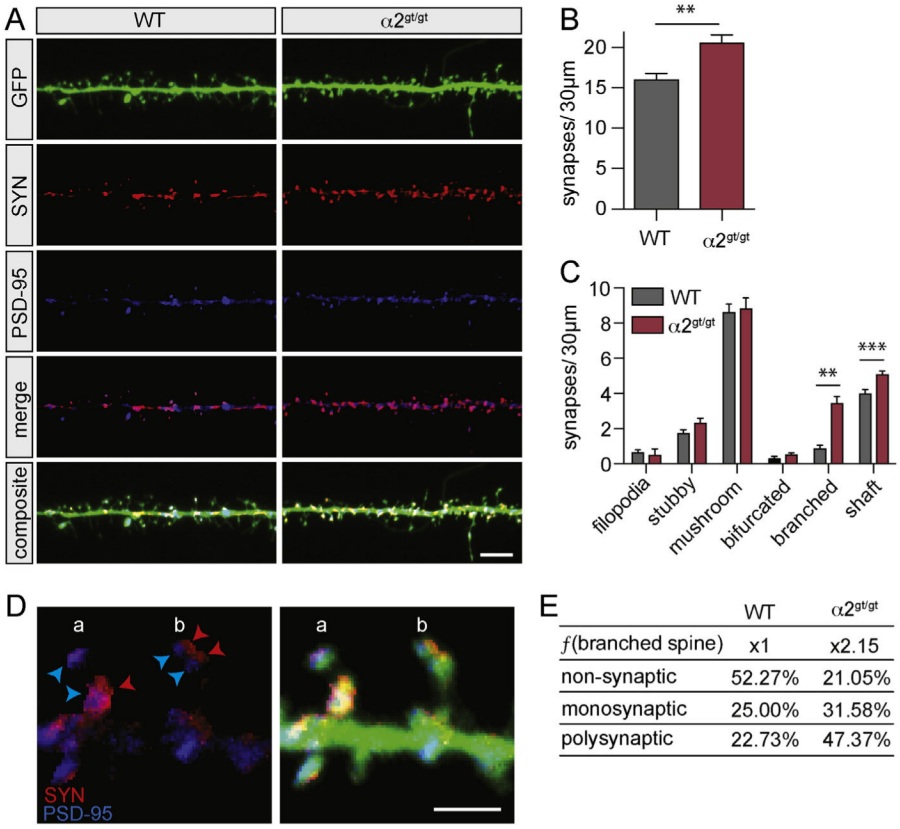

	WT	α2gt/gt
f(branched spine)	x1	x2.15
non-synaptic	52.27%	21.05%
monosynaptic	25.00%	31.58%
polysynaptic	22.73%	47.37%

Fig. 6.

The loss of α2-chimaerin alters synaptic contacts. (A) Representative images of 16 DIV WT and $\alpha2^{gt/gt}$ mutant dendritic segments expressing GFP, and immunostained with synaptophysin (red) and PSD-95 (blue). Scale bar equals 5 µm. (B) $\alpha2^{gt/gt}$ mutant hippocampal neurons exhibit an increase in synaptic contact density. Quantification of synaptic contact density (mean ± SEM/30 µm): WT = 16.00 ± 0.087 (n = 544), N = 3 experimental sets, 28 cells, 45 segments (30 µm) vs. $\alpha2^{gt/gt}$ = 20.56 ± 1.069 (n = 699), N = 3 experimental sets, 24 cells, 45 segments (30 µm). Unpaired two-tailed *t-test*, $^{**}p = 0.0011$. (C) $\alpha2^{gt/gt}$ mutants exhibit increased synaptic contacts formed on branched dendritic spines and the dendritic shafts. Quantification of synaptic contacts/spine type (mean ± SEM/30 µm): *filopodia*: WT = 0.617 ± 0.174 (n = 21) vs. $\alpha2^{gt/gt}$ = 0.470 ± 0.380 (n = 16), $p = 0.724$; *stubby*: WT = 1.70 ± 0.218 (n = 58) vs. $\alpha2^{gt/gt}$ = 2.294 ± 0.295 (n = 78), $p = 0.112$; *mushroom*: WT = 8.58 ± 0.499 (n = 292) vs. $\alpha2^{gt/gt}$ = 8.82 ± 0.612 (n = 300), $p = 0.766$; *bifurcated*: WT = 0.264 ± 0.160 (n = 9) vs. $\alpha2^{gt/gt}$ = 0.500 ± 0.114 (n = 17), $p = 0.237$; *branched*: WT = 0.852 ± 0.199 (n = 29) vs. $\alpha2^{gt/gt}$ = 3.411 ± 0.428 (n = 116), $^{**}p = 0.001$; *shaft*: WT = 3.970 ± 0.263 (n = 135) vs. $\alpha2^{gt/gt}$ = 5.058 ± 0.219 (n = 172), $^{***}p < 0.002$. WT: $N = 3$ experimental sets, 28 cells, 45 segments (30 µm), and $\alpha2^{gt/gt}$: N = 3 experimental sets, 24 cells, 45 segments (30 µm). Statistical significance determined using *t-test*, Holm-Sidak, $\alpha = 0.05$. (n = total # spines analyzed). (D) Representative image of multiple synaptic contacts on branched spines. Synaptophysin (SYN, red arrowhead) and PSD-95 (blue arrowhead) staining is shown. *Left*, monosynpatic branched spines (a) exhibit one spine head with SYN/PSD-95 apposition, while the other spine head is SYN positive, but PSD-95

negative. Polysynaptic branched spines (b) show two apposed SYN/PSD-95 puncta. *Right*, composite image of the same dendritic segment showing GFP-fill of the branched spine heads. Scale bar equals 2 μm. (E) Data table displaying the percentage of branched spines that exhibit monosynaptic, polysynaptic connectivity or are non-innervated. Alpha2-chimaerin mutants exhibit a significant difference in branched spine innervation compared to controls. WT: N = 3 experimental sets, 28 cells, 45 dendritic segments (30 μm) vs. $\alpha 2^{gt/gt}$: N = 3 experimental sets, 24 cells, 45 dendritic segments (30 μm). Fisher's exact test, two-tailed, $\alpha = 0.05$, $p = 0.003$.

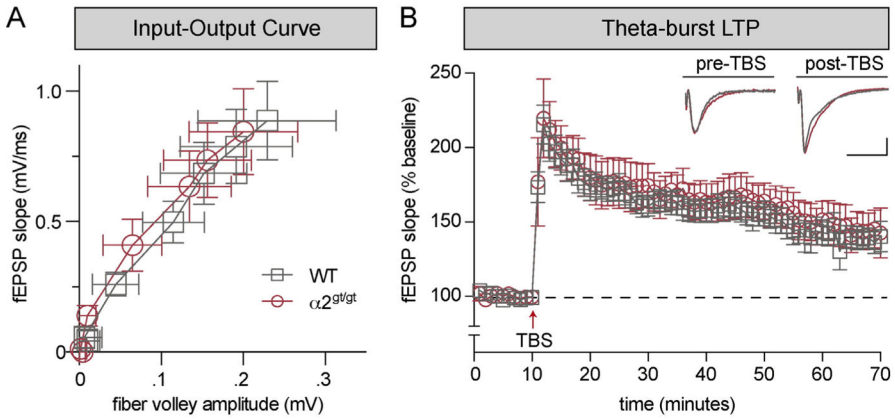

Fig. 7.

CA3-CA1 hippocampal synaptic efficacy is neither compromised, nor potentiated in α2-chimaerin mutants. (A) The loss of α2-chimaerin does not alter synaptic transmission. Input–output curve plotting the field excitatory postsynaptic potential (fEPSP) against fiber volley amplitude (mean ± SEM). Recordings were made from acute hippocampal slices from 5 to 6 month old mice: WT: N = 7 animals, n = 12 slices, vs. $\alpha2^{gt/gt}$: N = 7 animals, n = 18 slices. (B) LTP is not affected in $\alpha2^{gt/gt}$ mutant mice. LTP was induced by theta burst stimulation (red arrow) at 100 Hz (5 sweeps of 4 pulses delivered every 10 msec.) in the CA1 region of acute hippocampal slices from $\alpha2^{gt/gt}$ mutant and WT mice. Representative fEPSP recordings before and 60 min after LTP induction are displayed for WT (grey) and α2-chimaerin mutants mice (red). Scale bar is 1.4 mV, 30 msec. The fEPSP slope (mean ± SEM) is graphed during the time course of recording. Recording derived from 5 to 6 month old mice: WT: N = 7 animals, n = 12 slices and $\alpha2^{gt/gt}$: N = 7 animals, n = 18 slices.